JOURNAL OF MATERIALS SCIENCE 25 (1990) 4571–4578

Characterization of edge effects in cellular materials

R. BREZNY, D. J. GREEN
The Pennsylvania State University, Department of Materials Science and Engineering Ceramics Section, University Park, Pennsylvania 16802, USA

Cellular solids constitute a unique class of materials possessing a high stiffness to weight ratio. Due to the high level of porosity in these materials (70 to 99.7%) one must utilize special testing considerations in order to obtain accurate results. One of these items has been referred to as edge effects and stems from the large scale macrostructure of cellular materials. This results in a dramatic decrease in the mechanical properties when testing small specimens having a large cell size. A reticulated vitreous carbon was used to characterize these effects for both elastic modulus and flexural strength measurements. It was observed that a critical specimen to cell size ratio is required to overcome these effects and achieve accurate results. A simple model is presented to help in predicting these edge effects.

1. Introduction

There are a variety of porous, cellular materials which are most commonly, polymer foams. These are exploited for their specific stiffness in structural sandwich panel applications, where they are laminated between two dense materials as a means of maximizing the moment of inertia with a minimum of material. Another very important application of polymer foams is in packaging materials [1, 2]. Cellular ceramics have primarily been utilized for filtering molten metals. There may be, however, a wide range of structural applications for these ceramics which have not yet been realized. Cellular metals have been laminated with dense layers on the outer surface and assembled into structures such as mirrors and energy collection systems on satellites [3]. Their higher stiffness means that cellular ceramics have also drawn attention for these types of aerospace applications. Another possibility would be to use open cell ceramics as a skeleton to make mutually interconnected composites with other materials such as polymers or metals, i.e., both phases are three dimensionally connected. Irrespective of the specific application, the fundamental mechanical behaviour of the cellular structure must be understood.

Porous materials are found in a variety of microstructural types, one of these has been termed cellular. These cellular materials have a relative density less than 0.3 and are often represented by a repeating unit cell [2]. The cellular geometry may be two dimensional, e.g. honeycombs, or three dimensional, e.g. foams (Figs 1 and 2). Foams, have relatively isotropic cells and the mechanical properties mimic this behaviour. These materials are further classified into open and closed cell geometries. In open cell materials, the cells are interconnected such that there is a continuous pore phase throughout and the solid is an interconnected array of struts. Closed cell materials, on the other hand, have a thin membrane of solid in the cell faces sealing them from neighbouring cells.

The discrete nature of the microstructure in these materials, their irregular surfaces, and their mechanical fragility poses a whole set of questions in terms of mechanical testing requirements. For example, the strength of these materials in compression is about equal to that in tension and therefore crushing of the material at the load points or grips is of specific concern, especially as the applied stress is being amplified in the individual struts. It has been pointed out in indentation tests, one needs to consider carefully the probability of surface contacts [2]. Another important effect that results from the large scale macrostructure in these materials, is the requirement for a relatively large specimen size for testing, in order to obtain accurate property measurements. These are often referred to as edge effects. The impetus for this work was to evaluate the source of these edge effects and determine the specimen size required for a given cell size in order to obtain reliable results in bend testing. A simple model was also developed to predict the magnitude of these effects. It may also be possible to use this model to correct experimental strength values for these edge effects and obtain more reliable design data.

2. Experimental procedure

The material used in this study was a reticulated vitreous carbon*. Amorphous carbon is an ideal model material for studying the behaviour of brittle cellular solids such as ceramics. This material is fabricated by converting an open cell polymer foam into a glassy carbon by heating in an inert atmosphere. An

*Energy Research and Generation, Oakland, California 94608, USA.

0022–2461/90 $03.00 + .12

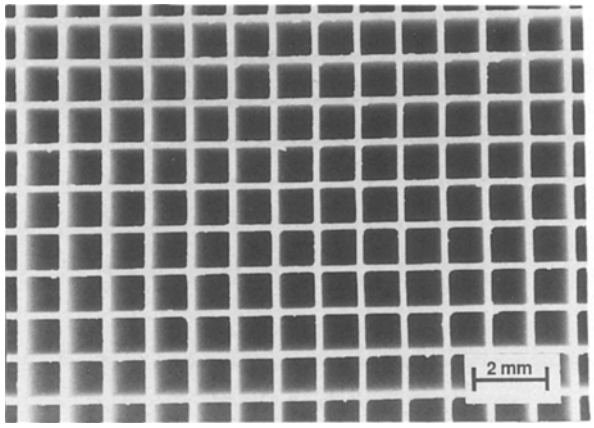

Figure 1 Microstructure of a two-dimensional honeycomb ceramic made up of square prismatic cells.

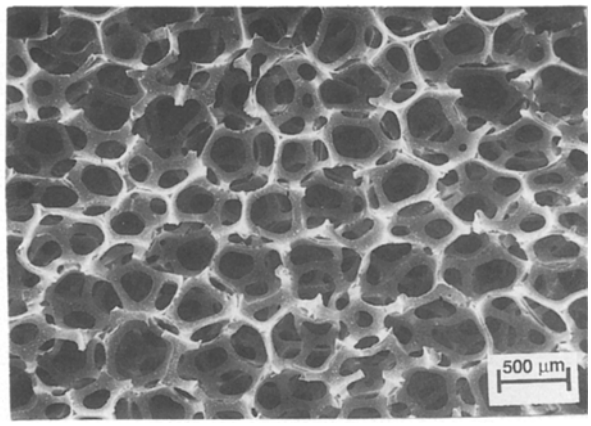

Figure 2 Microstructure of a three-dimensional reticulated vitreous carbon consisting of relatively isotropic open cells.

important aspect of this material is that the cells remain completely open down to the smallest cell sizes. Specimens were tested at three different cell sizes; 2.5, 0.56 and 0.25 mm and a relative density of approximately 0.035. The specimens consisted of beams of square cross-section and an aspect ratio of 5. Four or five specimen sizes were tested at each cell size in order to bracket a range of 2 to 100 cells being tested along the base and height of the sample. Table I shows the experimental matrix of specimen dimensions and cell sizes used in this study as well as the number of specimens tested under each condition.

The relative density of the specimens was determined from their weight and dimensions. A theoretical density of 1.49 g cm^{-3} was used for the solid vitreous carbon as suggested by the manufacturer. All of the specimens at a particular cell size were cut from the same billet of material to minimize specimen to specimen variability.

The Young's modulus was measured by the static technique in three-point bending. Five specimens at each condition were tested by measuring the load–deflection response and calculating the elastic modulus using [4]

$$E = (PL^3)/(4\delta_0 bh^3) \quad (1)$$

TABLE I Experimental matrix

Cell size (mm)	Specimen size (mm)	Cells along edge	Flexure span (mm)	Samples tested
2.5	50 × 50 × 250	20	230	5
2.5	38 × 38 × 190	15	165	10
2.5	25 × 25 × 127	10	115	20
2.5	13 × 13 × 64	5	54	20
2.5	5 × 5 × 38	2	32	20
0.56	38 × 38 × 229	70	210	10
0.56	25 × 25 × 127	45	115	20
0.56	15 × 15 × 76	25	63	20
0.56	6.4 × 6.4 × 38	10	32	15
0.56	5 × 5 × 38	5	32	20
0.25	25 × 25 × 127	100	115	20
0.25	18 × 18 × 89	70	79	20
0.25	10 × 10 × 51	40	45	20
0.25	5 × 5 × 38	10	32	20

*Instron Corporation, Canton, Massachusetts 02021, USA.

where P is the load, δ_0 the maximum deflection, L the span of the fixture and b, h the base and height of the specimen, respectively. The load was applied using a mechanical testing apparatus* and the deflection was measured optically using a horizontally mounted stereomicroscope equipped with a calibrated eyepiece. Deflections as small as 6 μm could be measured accurately giving a maximum error of $\pm 5\%$ in the deflection measurements. The shear contribution to the deflection was calculated as being a maximum of 10% and therefore was not accounted for in the analysis. The loads which were required to deflect the smallest specimens were less than that detectable by the load cell. In this case a pan balance was used to measure the load. The elastic modulus of several samples was verified using the resonance technique [5] and gave good agreement with the static measurements.

The bend strength was determined using the same three-point bend fixtures as in the modulus measurements. This configuration was selected to minimize crushing of the specimen beneath the load points. Due to the low hardness of glassy carbon, small pieces of cardboard reinforced with glass slides had to be placed at the load points to distribute the load and prevent crushing. Teflon cylinders were used as the load supports in order to minimize friction during testing. The equation used to calculate the bend strength of a rectangular beam subjected to three-point bending is given as

$$\sigma_f = (3PL)/(2bh^2) \quad (2)$$

where the variables have the same meaning as in Equation 1.

3. Results

Scanning electron micrographs of the material (Fig. 2) shows the three-dimensional cell geometry and the smooth, dense, glassy surface of the solid material. This photomicrograph is of the finest cell size (0.25 mm) sample showing a completely open cell structure. In Fig. 3 the fracture surface of an individual strut exhibits a fracture pattern characteristic of an amorphous, brittle material. This fracture surface also shows that the struts in this material are fully

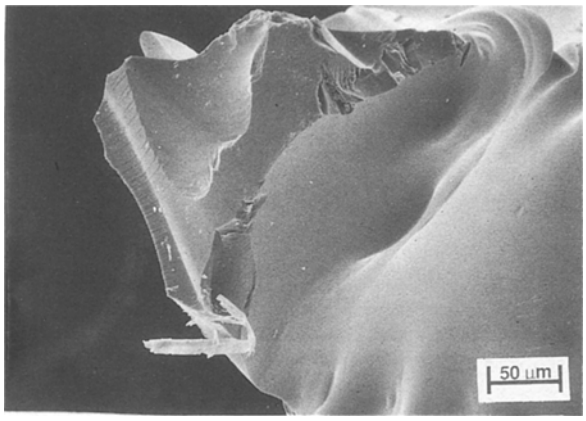

Figure 3 Fracture surface of an individual solid strut exhibiting brittle conchoidal fracture.

dense throughout. This is different from the hollow struts which result when cellular ceramics are fabricated by coating a polymer substrate with a ceramic slurry. The subsequent removal of the polymer prior to sintering of the ceramic results in a large triangular hole down the centre of the struts [6].

The elastic modulus and bend strength results are summarized in Table II. The density of the specimens varied from 3.0 to 4.0% of the theoretical value. The specimen to cell size ratio indicates the number of cells which are along the base and height of the samples. Both the strength and modulus remain fairly constant at large specimen sizes where they reach a plateau value. At smaller specimen sizes both properties appear to decrease dramatically with size. We can argue that to a first approximation, the true strength and stiffness of the cellular material is not expected to change with specimen size. The apparent reduction with decreasing specimen size that is observed in Table II is a result of not considering edge effects i.e., the calculated properties, based on the measured sample dimensions, significantly underestimated the true properties of the material. The properties measured for the large specimens are more representative of the true material properties because the contribution of the edge effects is within the other experimental errors involved in the tests. Certainly the larger the specimen to cell size, the more closely the material approaches a continuum. Based on these results, one should test samples having at least 15 to 20 cells along the base and height of a bend specimen in order to minimize these effects and obtain reliable data for the actual strength of these materials. In large cell materials, testing very large samples is not always practical and, therefore, one may prefer to correct for these edge effects. On this basis, the following model is proposed, which indicates the source of the edge effects.

4. Edge effects model

Edge effects stem from the large scale macrostructure of most cellular materials and become important at small specimen size to cell size ratios. It is proposed that edge effects are a result of a poorly connected, outer surface region. Cutting, machining or other forms of surface damage of these materials could enhance this damaged region. These outer cells are included in the specimen dimensions, however, contribute little to the properties of the sample. The way in which this layer of cells will affect the properties depends on the loading geometry used in the test. For example, under axial loads this outer layer of cells will result in a reduction in the effective cross sectional area of the sample which is carrying the load. Under bending stresses, on the other hand, this layer of cells results in a decrease in the effective moment of inertia of the beam. At small specimen to cell size ratios, the surface cells constitute a large fraction of the specimen cross-section and it is in these specimens that edge effects dominate the test errors. These effects may play a significant role in all property measurements which rely on the sample dimensions to obtain the stressed volume of material. In cellular solids, particularly at small specimen sizes, this outer layer of poorly connected cells makes it very difficult to accurately obtain this stressed volume.

This work has concentrated on understanding the edge effects under bending stresses and their effect on elastic modulus and bend strength measurements. In

TABLE II Mechanical property results

Sample (mm)	Cell size (mm)	Specimen size / Cell size	Relative density	Elastic modulus (MPa)		Bend strength (MPa)	
				Average	Standard deviation	Average	Standard deviation
50 × 50 × 250	2.5	20	0.032	49.0	3.61	0.793	0.097
38 × 38 × 190	2.5	15	0.031	52.4	3.68	0.772	0.078
25 × 25 × 127	2.5	10	0.031	41.3	5.48	0.771	0.065
13 × 13 × 64	2.5	5	0.027	30.3	2.88	0.689	0.099
5 × 5 × 38	2.5	2	–	2.44	1.16	0.129	0.071
38 × 38 × 229	0.56	70	0.035	63.3	5.13	0.812	0.112
25 × 25 × 127	0.56	45	0.036	59.9	9.30	0.952	0.087
15 × 15 × 76	0.56	25	0.035	34.4	5.50	0.686	0.121
6.4 × 6.4 × 38	0.56	10	0.036	33.3	6.56	0.720	0.162
5 × 5 × 38	0.56	5	0.029	8.28	2.97	0.229	0.115
25 × 25 × 127	0.25	100	0.041	53.5	5.20	1.27	0.060
18 × 18 × 89	0.25	70	0.040	40.7	3.21	1.28	0.054
10 × 10 × 51	0.25	40	0.041	42.3	1.61	1.24	0.103
5 × 5 × 38	0.25	10	0.036	36.4	2.41	1.08	0.097

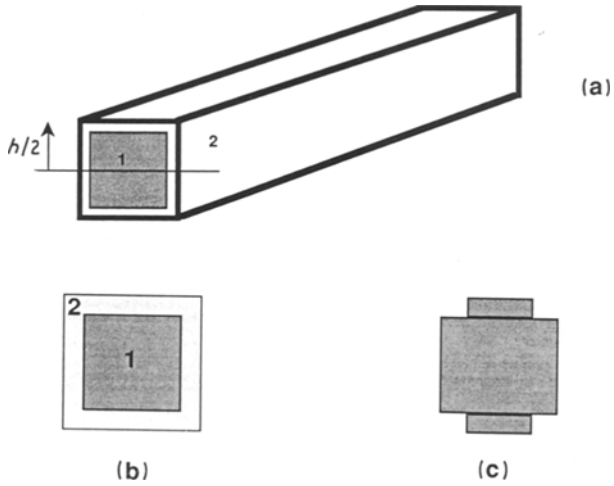

Figure 4 (a) Schematic of rectangular beam made up of two materials. (b) Unit cross section of beam having core of material 1 (modulus E_1) and an outer layer of material 2 (modulus E_2 where $E_2 < E_1$) having thickness X. (c) Transformed cross-section made up entirely of material 1 but maintaining the same resistance to bending as Fig. 4b.

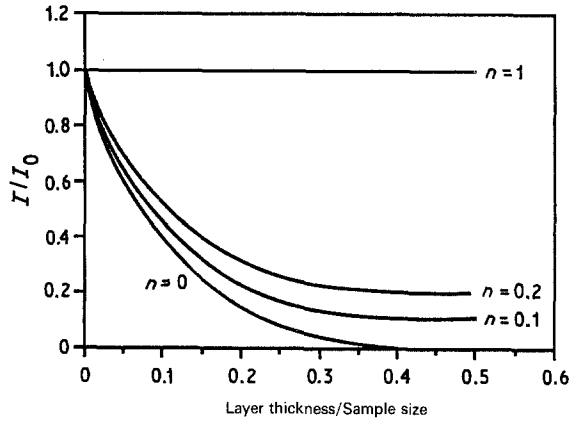

Figure 5 Relative moment of inertia, as predicted by the model, plotted against the ratio of the outer layer thickness and the base or height of the beam. Shown are curves for different values of $n = E_2/E_1$.

beam bending theory, the stiffness of a beam can be described in terms of its load–deflection response by the expression [4]

$$E = (PL^3)/(48\delta_0 I) \quad (3)$$

where clearly a primary factor affecting the modulus is the moment of inertia of the beam. The stresses in a continuum beam subjected to bending are described by the expression:

$$\sigma = My/I \quad (4)$$

where M is the bending moment and y the distance from the neutral axis to a point of stress within the beam. For linearly elastic materials, the stress profile through the beam is linear. Based on this relationship, it is clear that the strength calculation is not only affected by the reduction in the effective moment of inertia but also a reduction in the distance y as a result of having a poorly connected layer of cells at the surface of the sample.

It may be possible to predict these edge effects using a simple technique based on the bending of composite beams. If one considers a rectangular beam having a unit cross-section being made up of two materials with different elastic moduli as shown in Figs 4a and b. Region 1 consists of the cellular material where all of the cells are intact and has a modulus E_1 and region 2 is the layer, around the outside of the beam, where the cells are poorly connected. The outer layer, of thickness X, has a lower modulus (E_2) then the undamaged material. The ratio of the two moduli is represented by the factor $n = E_2/E_1$ where in these materials n is always less than 1. One can make the entire beam of one modulus (E_1), and still maintain the same resistance to bending, by multiplying the width of each element of modulus E_2 by the factor n. The narrowing of the sections must be made in a direction parallel to the neutral axis of the beam so that the distance y of each section from the neutral axis remains the same. The transformed cross-section, assuming $n = 0.5$, is shown in Fig. 4c. The parallel axis theorem can be used to calculate the moment of inertia of this transformed beam in terms of the moments of inertia of each section [4]. Assuming a beam of unit cross-section, the moment of inertia of the transformed section (Fig. 4c) is given by

$$I = [(1 - 2nX)(1 - 2X)^3/12] + [2nX^3/12] + [nX(1 - X)^2] \quad (5)$$

where X is the thickness of the poorly connected outer layers of modulus E_2. In this expression the first two parts describe the moment of inertia of the three sections about their respective neutral axes and the last part transfers the moment of inertia of the two small rectangles to the parallel axis of the transformed beam. A plot of the relative moment of inertia against layer thickness is shown in Fig. 5. I is the moment of inertia of the transformed beam as given by Equation 5 and I_0 is the moment of inertia of the simple rectangular beam (Fig. 4b) made entirely of material 1. This latter beam assumes that no edge effects are involved as assumed in the original testing procedure and the use of Equations 1 and 2. At thin layers the moment of inertia drops very rapidly as a result of having the lower modulus material at the surface, and becomes almost constant at a layer thickness which is 20% of the beam height. This corresponds to a beam having 64% of the original cross section made up of disconnected cells. The relative moment of inertia of the beam finally levels off asymptotically at a value equal to the modulus ratio of the two materials. This type of simple model may be useful in describing the edge effects in brittle open cell materials.

5. Discussion of results

The experimental elastic modulus results are plotted as the relative modulus (E/E_0) against the specimen to cell size ratio in Fig. 6. The relative modulus is described as the experimental modulus of the sample (E) divided by the modulus of the same cell size material but exhibiting little or no edge effects (E_0). The value of E_0 was taken as the average value of the large specimens where the modulus reached a relatively constant value. The moduli contained in this plateau region were determined as those having a statistically

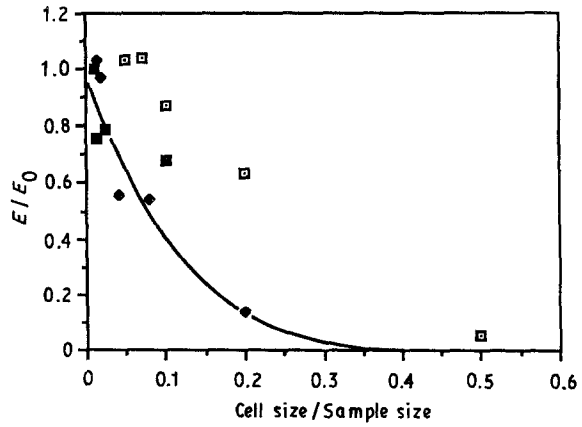

Figure 6 Experimental results of the three different cell size materials plotted as the relative elastic modulus against the ratio of cell size and the base or height of the samples. Also included is theoretical line given by model. (□ 2.5 mm, ◆ 0.56 mm, ■ 0.25 mm, —— model.)

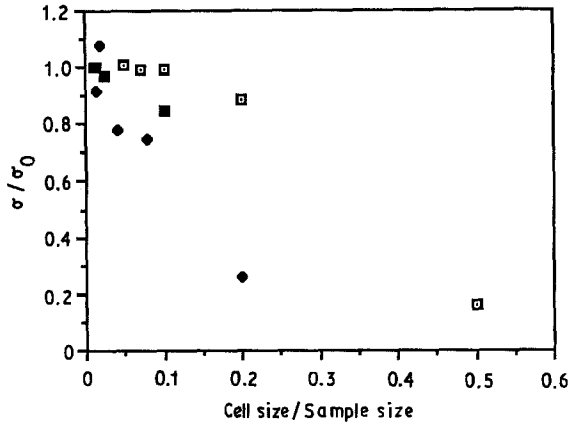

Figure 7 Experimental results for the three materials plotted as the relative strength against the ratio of cell size over sample size. (□ 2.5 mm, ◆ 0.56 mm, ■ 0.25 mm.)

insignificant difference between their means at a significance level of 0.05. Since the elastic modulus of a beam, subjected to bending, scales directly with the moment of inertia, one would expect similar behaviour to that given by the model in Fig. 5. A theoretical line, given by the model, was selected to give a best fit to the majority of the data and is included in Fig. 6. This line corresponds to a modulus ratio (n) value very close to 0 and a value of X equal to the cell size. The data exhibits the general trend of decreasing modulus with specimen size as described by the model and the 0.56 and 0.25 mm cell size specimens give a reasonable fit to this theoretical line. The large cell material (2.5 mm) exhibits the same trend, however, the points are shifted to the right of the theoretical line. Perfect agreement of the measured values with the model is only possible if the thickness of the poorly connected layer of cells would equal the cell size. The fact that the large cell data is shifted to the right of the predicted line indicates that the layer thickness in these samples is less than the cell size. It may be more realistic to treat the outer, poorly connected layer as a damage zone that may include other effects such as damage from the cutting and machining operations. In this case, the depth of this damage zone would be controlled by a balance between the magnitude of the stress field induced by the machining operation and the strength of the individual struts within the structure. Based on this argument, it is feasible that the thickness of this damage zone be greater than one cell size in small cell materials, if the stress field required for strut failure extends beyond one cell diameter. In large cell materials, a damage zone less than one cell size is equally possible, as the cells are arranged randomly within the structure and therefore, the edge of a cell will occur at a mean depth of approximately half the cell size from the outer surface.

It may be possible to use the type of plot shown in Fig. 6 to estimate the thickness of this damaged zone by comparing the experimental values with the theoretical line. One must realize, however, that this is an estimated thickness averaged over the entire specimen surface and in reality may not be as uniform as depicted by the model (Fig. 4a). In reality, the thickness of this layer will vary from point to point along the surface of the sample about a mean value as estimated by the model.

The relative strength is plotted in the same manner in Fig. 7. A similar trend to that seen in the modulus data is observed for smaller specimens. In terms of the model, the calculated values of the strength are reduced due to both a reduction in the effective moment of inertia, as well as, a change in the location of the point of maximum stress within the beam. It may be possible to account for this large variation in the calculated strength as a result of edge effects by using the proposed model. From Equation 3, the elastic modulus is proportional to the moment of inertia of a linearly elastic beam. The stress also depends on the moment of inertia (Equation 4) and scales linearly with the distance from the neutral axis to the point of maximum stress (y) within the beam. The failure strength is usually taken as the value of the maximum tensile stress occurring at a distance furthest from the centroid of the beam. Equation 3 can be rearranged to give the moment of inertia in terms of the load–deflection response of the sample

$$I = (PL^3)/(48E_0\delta_0) \quad (6)$$

This represents the effective moment of inertia of the sample and can be substituted into Equation 4, i.e., we are assuming that we need to measure I rather than calculating a value from the beam dimensions. The strength can be further corrected by utilizing the estimated damage zone thickness to account for the change in y due to the presence of this damaged layer of cells. This yields an expression for the bend strength which has been corrected for edge effects; i.e.,

$$\sigma = \{12\delta_0 E_0[(h/2) - X]\}/L^2 \quad (7)$$

where δ_0 is the maximum deflection at fracture, E_0 the true elastic modulus of the cellular material.

The measured strength values for all the specimen sizes have been treated using this approach and are plotted in Fig. 8. Correcting for the edge effects has resulted in a dramatic reduction of the variability in the strength values over those plotted in Fig. 7 and shows that the strength is relatively independent of specimen

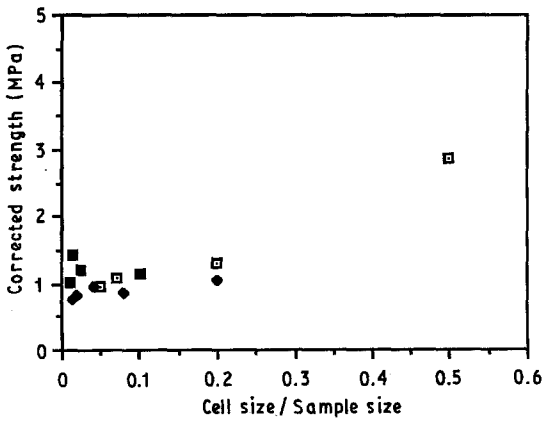

Figure 8 Experimental values of the strength corrected for edge effects by the simple model and plotted against cell size over sample size. (□ 2.5 mm, ◆ 0.56 mm, ■ 0.25 mm.)

size. The variability has been reduced from an order of magnitude to a factor of 2. As will be discussed later, this remaining variability may be related to the uncertainty in estimating the stressed volume in small specimens. Some scatter in the strength is still observed which may be attributed to experimental errors, errors in the model assumptions or differences in the carbon properties from specimen to specimen. The deviation in the average value plotted at a cell—specimen size ratio of 0.5 is attributed to error in accurately measuring the sample dimensions as these specimens consisted of only 1 to 2 cells across the base and height. This data set also had an extremely large variance.

It is important to point out that there is an additional factor not accounted for in this analysis which results from the statistical nature of flaws in ceramics. In dense ceramics the strength shows an inverse dependence on the sample volume due to the reduced probability of finding a critical flaw in a smaller volume of material. Dense ceramics therefore exhibit an increase in strength with decreasing specimen size for a constant flaw distribution. In the range of specimen sizes included in this study this behaviour is overshadowed by the edge effects. For example, assuming a two-parameter Weibull distribution having a Weibull modulus of 15, which is typical for these materials, an order of magnitude decrease in sample volume would be predicted to give a 16% increase in strength from [7]

$$\sigma_1/\sigma_2 = (V_2/V_1)^{1/m} \quad (8)$$

where m is the Weibull modulus, σ_1 and σ_2 the fracture stresses of the two samples and V_1, V_2 are their respective volumes [7]. This expression assumes the same loading geometry for both specimen sizes. For most ceramic materials, where edge effects do not significantly alter the stressed volume, the volume effect given by Equation 8 dominates the specimen size behaviour. One might expect these probabilistic effects to dominate in very large cellular specimens as well, where edge effects become insignificant.

Thus far we have shown that testing specimens which are too small can result in an underestimation of the true strength of the material. This was explained as resulting from an uncertainty in the volume of material being tested due to a poorly connected layer of cells over the sample surface. When designing with ceramics it is not only important to know the magnitude of the strength but also the width of the strength distribution. In this study, the variability in the strength increased significantly when testing the small specimen sizes. This is believed to be a result of the uncertainty in knowing the stressed volume of material at small specimen to cell size ratios. Specimen sizes were selected such that at least 15 to 20 samples were tested in the group and a damage zone was predicted by the simple model. The strengths for these samples are shown in Table III, as well as, the coefficient of variability which is defined as the standard deviation of the data divided by the mean. It was observed, in both the calculated strength, as well as, that corrected by Equation 7, that the coefficient of variability increases with decreasing specimen size. Based on a statistical approach to the strength distribution, if the damage zone was of a uniform thickness over the entire sample surface, the coefficient of variability should not change with specimen size. In reality, however, the damage zone varies from point to point along the sample about some mean value which is predicted by the model. The thickness of the damage zone was estimated from the average elastic modulus of five samples whereas the strength was measured on 20 samples and, therefore, the strength correction was unable to account for this variability. It is felt that the

TABLE III Strength variability analysis

Sample (mm)	Cell size (mm)	Bend strength (MPa)		Corrected strength (MPa)		Coefficient of variability (based on $1/bh^2$)
		Average	Coefficiency variability	Average	Coefficiency variability	
25 × 25 × 127	2.5	0.771	0.084	0.839	0.122	0.035
13 × 13 × 64	2.5	0.689	0.144	0.916	0.149	0.120
5 × 5 × 38	2.5	0.129	0.550	0.969	0.631	0.300
25 × 25 × 127	0.56	0.952	0.091	0.832	0.136	0.011
15 × 15 × 76	0.56	0.686	0.176	0.959	0.174	0.150
6.4 × 6.4 × 38	0.56	0.720	0.225	0.867	0.400	0.173
5 × 5 × 38	0.56	0.229	0.502	1.060	0.491	0.581
18 × 18 × 89	0.25	1.28	0.058	1.67	0.059	0.069
10 × 10 × 51	0.25	1.24	0.083	1.52	0.158	0.056
5 × 5 × 38	0.25	1.08	0.090	1.44	0.432	0.103

increase in the strength variability is due to the uncertainty in the stressed volume of the beam and as the specimen size decreases, the fraction of the volume composed of this damaged region constitutes a significant portion of the sample.

A simple approximation was used to estimate the variability in the sample volume and was compared to the strength variability. In the calculation of strength (Equation 2), the fracture load and span of the fixture are known with reasonable accuracy and therefore contribute very little to the total error in the strength calculation. The largest portion of the variability, other than that predicted by flaw statistics, results primarily from the uncertainty in the bh^2 term in the denominator. We can estimate the mean and standard deviation of b and h if we assume that they follow a normal distribution. The model proposed in this paper predicted an average value of the damage zone, and from the sample dimensions we know the maximum possible values of b and h. If the specimen dimensions fit a normal distribution then on each surface, b is centred about a mean value with one damage zone thickness (X) above it and one below it. As there are two surfaces, the mean value of b can be estimated as $\bar{b} = b - 2X$. From the Empirical Rule we know that approximately all of the measurements fitting a normal distribution are within three standard deviations from the mean [8]. We can then estimate the population standard deviation, $\sigma_b \cong 2X/3$. The specimens used in this study had a square cross-section ($b = h$) and, therefore, both dimensions have approximately the same mean and variance. Multiplicative rules of statistics allow one to predict the variance of a product of two independent normal random variables if their respective means and variances are known [9]. Although we know the distributions of b and h, we do not know how their reciprocals are distributed. We cannot, therefore, use these statistical relationships to estimate the variance in strength as a function of the variance in $1/bh^2$. It is possible to estimate this through simulation. This was done by randomly generating 5000 numbers fitting a normal distribution having the mean and standard deviation of b and h as described above. One can then take the reciprocal of the cube of these numbers and calculate the mean and standard deviation of this transformed data set. The coefficient of variability of these transformed values should give an estimate of the coefficient of variability in the strength due to the uncertainty in $1/bh^2$. This simulation was performed for the specimen sizes in Table III and the results are given in the last column. Comparing the coefficients of variability in $1/bh^2$ with those of the experimental bend strength data it appears that the majority of the variability in the strength measurements can be accounted for by the uncertainty in the actual stressed volume of material. The same increasing variability is observed in the dimensions and the strength with decreasing specimen size.

Strength variability is often discussed using a Weibull analysis where the Weibull modulus, m, describes the width of the strength distribution. The Weibull modulus is commonly used in the design of structural components to maintain a certain maximum risk factor for catastrophic failure. If one relates the standard deviation of the data to a Weibull modulus for the large specimens, where minimal edge effects are incurred, a value for m in the range of 15 to 25 is typical for these materials. At the smaller specimen sizes, where the uncertainty in sample volume contributes to a broader strength distribution, the Weibull modulus quickly drops to 2 to 6. This indicates that it is important to test large specimen sizes of cellular materials because the edge effects lead to an underestimation of the magnitude of the strength, as well as, an overestimation of the width of its distribution. One can use the proposed model to account for edge effects in small specimens, however, a large number of specimens must be tested to obtain an accurate estimate of the mean. This is due to the increased variability resulting from the uncertainty in the stressed volume of small specimens. In order to precisely describe the width of the strength distribution one must test large specimen sizes.

6. Summary and conclusions

This work involved the measurement of the elastic modulus and strength of a reticulated vitreous carbon to study the edge effects on the properties of brittle cellular materials. It was shown that in a three-point bend geometry these materials can exhibit significant edge effects when small specimen sizes are tested. These edge effects stem from the relatively large macrostructure found in cellular solids which results in a poorly connected layer of cells at the surface of the samples. This layer of poorly connected cells is included in the total sample volume but contributes very little to the mechanical properties. The effective moment of inertia, as well as, the distance from the neutral axis to the point of maximum stress in the beam is less than expected based on the sample dimensions. This results in a dramatic underestimation of the magnitudes of the material properties and an overestimation of the width of their distributions when calculated using standard beam equations. It was observed that samples which are tested in bending must have at least 15 to 20 cells along the base and height in order to minimize these effects.

A simple model, based on a composite beam analysis, was proposed as a way to correct for these edge effects when the testing of large specimens becomes impractical. Experimentally this involves the incorporation of a deflection measurement during the strength testing procedure. The load–deflection response of the sample is then used to estimate the thickness of the damaged zone and the reduced moment of inertia due to this outer damaged layer of cells. It was found that this type of treatment can reduce errors in bend strength measurements from an order of magnitude to less than a factor of two. When working with new classes of materials, like cellular solids, it is important to realize these types of special testing considerations particularly when relying on laboratory samples to obtain characteristic material properties.

Acknowledgements

This work was supported by the National Science

Foundation under grant No. DMR-8603878. We acknowledge the students and staff of the Materials Science and Engineering Department who assisted in this study. Special thanks is extended to Sam Salamone for his assistance in the testing of these materials, as well as, Bryan Leyda and John O'Connor of ERG Inc. for supplying the samples used in this study.

References

1. M. F. ASHBY, *Metall. Trans.* **14A** (1983) 1755.
2. L. J. GIBSON and M. F. ASHBY, "Cellular Solids, Structure and Properties" (Pergamon Press, Oxford, UK, 1988).
3. B. LEYDA, Personal communications.
4. F. P. BEER and E. R. JOHNSON, "Mechanics of Materials" (McGraw Hill, New York, 1981) pp. 582–583.
5. W. R. DAVIS, *Trans. Brit. Ceram. Soc.* **67** (1981) 515–541.
6. R. BREZNY, D. J. GREEN and C. Q. DAM, *J. Amer. Ceram. Soc.* **72** (1988).
7. G. J. DESALVO, Westinghouse Electric Corporation, Astronuclear Laboratory report number WANL-TME-2688 (1970).
8. L. OTT, "An Introduction to Statistical Methods and Data Analysis", 2nd Edn (Duxbury Press, Boston, MA, 1984).
9. M. H. DEGROOT, "Probability and Statistics" 2nd Edn (Addison-Wesley, Reading, MA, 1986).

Received 26 June
and accepted 1 December 1989